DENTAL MATERIALS 35 (2019) 356–367

Available online at www.sciencedirect.com

ScienceDirect

journal homepage: www.intl.elsevierhealth.com/journals/dema

Synergistic effects of VE-TPGS and riboflavin in crosslinking of dentine

U. Daood[a], J.P. Matinlinna[b], A.S. Fawzy[c,*]

[a] Clinical Dentistry, Restorative Division, Faculty of Dentistry, International Medical University Kuala Lumpur, 126, Jalan Jalil Perkasa 19, 57000 Bukit Jalil, Wilayah Persekutuan Kuala Lumpur, Malaysia

[b] Dental Materials Science, Applied Oral Sciences, Faculty of Dentistry, The University of Hong Kong, Prince Philip Dental Hospital, 34 Hospital Road, Sai Ying Pun, Hong Kong SAR, China

[c] UWA Dental School, University of Western Australia, 17 Monash Avenue, Nedlands, WA 6009, Australia

ARTICLE INFO

Article history:
Received 12 September 2018
Received in revised form
24 November 2018
Accepted 27 November 2018

Keywords:
Dentine
Collagen enhancer
Riboflavin
Crosslinking
Bond strength
Adhesion strength
Hybrid
Raman spectroscopy
TEM

ABSTRACT

Objective. Effect of D-alpha-tocopheryl poly(ethyleneglycol)-1000-succinate (VE-TPGS) with riboflavin-5′-phosphate solution on crosslinking of dentine collagen was investigated to analyze collagen's structural integrity.

Methods. VE-TPGS was added to RF-solution, at RF/VE-TPGS (*w/w*) ratios of 0.125/0.250 and 0.125/0.500. Demineralized dentine beams were used (10 wt.% phosphoric acid), rinsed using deionized-water and analysed using ELISA (Human MMP2 ELISA; Human CTSK/Cathepsin-K for MMP2 and Cathepsin K analysis). AFM of dentine collagen-fibrils structure was done before and after dentine specimens' placement in mineralization solution and tested after 14 days in artificial saliva/collagenase (AS/Co) solution. The specimens were tested after 24 h in mineralization solution for surface/bulk elastic modulus. Nano-indentation was carried out for each specimen on intertubular-dentine with lateral spacing of 400 nm. Reduced elastic-modulus and nano-hardness were calculated and collagen content was determined using hydroxyproline-assay. Micro-Raman were performed. TEM was carried out to study structural variations of dentine-collagen in artificial-saliva (collagenase). Data were presented as mean ± standard deviation and analyzed by SPSS v.15, by analysis of variance.

Results. Synergetic effect of VE-TPGS was observed with RF through higher structural integrity of dentine collagen-fibrils shown by TEM/AFM. Superior surface/bulk mechanical stability was shown by nano-indentation/mechanical testing. Improvement in collagenase degradation resistance for hydroxyproline release was observed and lower endogenous-protease release of MMP-2/Cathepsin-K. Raman-analysis analysed chemical interactions between RF and collagen confirming structural-integrity of collagen fibrils after crosslinking. After 24 h mineralization, AFM showed mineral depositions in close association with dentine-collagen fibrils with RF/VE-TPGS formulations.

Significance. Potential synergetic effect of RF/VE-TPGS was observed by reflection of higher structural integrity and conformational-stability of dentine-collagen fibrils.

* *Corresponding author.*
E-mail address: amr.fawzy@uwa.edu.au (A.S. Fawzy).

https://doi.org/10.1016/j.dental.2018.11.031

1. Introduction

Dentine forms the bulk of tooth-structure and its structural stability is crucial for restorative procedures [1]. Dentine adhesives associated with dentine collagen fibrils form the so-called hybrid-layer expected to withstand chemical and mechanical stresses. This hybrid layer where the adhesive intermingles with the collagen fibers is also considered as a weak link, prone to degradation by hydrolysis and host-derived proteinases [2,3]. Exposed denuded collagen fibrils are vulnerable to endogenous matrix metalloproteinases (MMPs) [4], cathepsin-K enzymes acting on C-terminally located cleavage site [5], and other enzymes from bacteria or saliva [6]. This failure of interface is considered pivotal in determining longevity of adhesive fillings due to disorganization of collagen fibrils [7]. Many self-etch and etch-and-rinse adhesive systems fail to completely infiltrate the demineralized fibrous network rendering exposure of collagen fibers [8]. It has previously been reported that preservation of collagen within the dentine matrix is essential for stability of the resin-dentine adhesion [9]. Suboptimal infiltration of denuded collagen fibrils is very common, especially as observed with etch-and-rinse adhesives [10,11] and to some extent with self-etch adhesives [12]. These denuded collagen fibrils are subjected to challenge by exogenous enzymes in saliva [13] and endogenous enzymes within the dental tissues, namely MMPs and cysteine cathepsins [14]. Degradation of collagen fibrils results in loss of helical structure and uncoiling into gelatin, leading to fragmentation of the collagen. Subsequently, gelatin becomes further degraded into amino acids by gelatinases or hydrolysis [15]. As a consequence, it has led to extensive research aiming to prevent collagenolysis in the hybrid layer.

Preservation of intact collagen fibril structure within dentine-matrix is essential for stability of resin-dentine bond [8]. Collagen cross-linkers have recently been investigated to enhance collagen degradation resistance and inactivate collagenolytic enzymes aiming to retain integrity of hybrid layer and prevent its degradation [16,17]. Inhibition of protease enzymes has been recommended previously through the use of synthetic MMP inhibitors, such as CHX, [18,19] quaternary ammonium methacrylates [20], or benzalkonium chloride (BAC) [21] The endogenous proteases present inside the dentine need to be inactivated in order to prevent proteolysis of the dentinal matrix. Crosslinking agents can affect remineralization processes serving as a non-invasive therapy [22].

Water-soluble riboflavin (RF), vitamin B_2, produces so-called singlet oxygen radicals ($^1O_2$) by ultraviolet-A (UVA) radiation thereby producing collagen cross-linking that creates covalent intermolecular cross-links via photo-oxidation. This was reported to enhance biomechanical properties and enzymatic degradation-resistance of collagen matrices inside corneal tissues [23]. Cross-linking using riboflavin formulations modified with chemical permeation enhancers was investigated aiming to enhance riboflavin uptake and accumulation by corneal collagen [24]. Several permeation enhancers were investigated, such as benzalkonium chloride (BAC) [25], gentamicin (an antibiotic), ethylenediamine tetraacetic acid (EDTA) [26], and D-alpha-tocopheryl poly(ethyleneglycol)-1000-succinate (VE-TPGS) [27]. Although the mechanism of such permeation enhancement is not fully clarified, it has been reported to enhance the uptake and corneal-accumulation of riboflavin-5′-phosphate which improved collagen crosslinking [23]. Vitamin-E TPGS (VE-TPGS) is a non-ionic surfactant known to act as riboflavin transporter through different biological barriers [28]. It also has a protective effect against free-radical damage associated with generation of reactive oxygen species during riboflavin photo-activation through quenching effect [29]. Along with this, remineralization is understood to take place by using different strategies such as by including fluoride (*e.g.* NaF), amorphous calcium phosphate $Ca_3PO_4)_2$, or bioactive glass (BAG). This improves the resistance of bonded restorations to secondary caries [30]. With the traditional ion-based strategies, however, remineralization fails where there is absence of seed crystallites [31].

The interaction of photo-activated riboflavin (from 0.1% to 1%) with dentine collagen-matrix [32] and resin-dentine interface [33] was investigated with promising results. However, with the use of riboflavin and other crosslinking agents, there was reduction of bond degradation and the degree of conversion was not jeopardized for adhesive polymerisation [34]. In the current study, we are investigating the synergetic effect of VE-TPGS coupled with riboflavin-5′-phosphate solution (0.125%) on the cross-linking of dentine collagen-matrices. Our interest was in: collagen structural integrity and conformational stability, chemical interactions, collagenase mediated degradation resistance, mechanical properties, remineralization-potential and endogenous proteases inhibition. The null hypotheses tested were included in the idea that VE-TPGS incorporation has no effect on the: (i) mechanical stability in terms of nano-indentation properties (such as h Hardness, H, and & reduced elastic-modulus, E_r), and bulk apparent elastic-modulus E_{appr}, (ii) inhibition of dentinal proteases in terms of MMP-2 and cathepsin-K, and (iii) biochemical stability in terms of hydroxyproline (HYP) release.

2. Materials and methods

Fifty-eight extracted human-molars (21–35 years) were used in this study and ethical approval was received from the Institutional Review Board, National University of Singapore. Riboflavin-5-phosphate (Sigma-Aldrich) was used as such and dissolved in distilled water to obtain 0.125% RF formulations and kept in light proof test tubes. Next, VE-TPGS was added directly to the RF-solution, at RF/VE-TPGS (*w/w*) ratios of [35]: 0.125/0.25 (RF/VE-$TPGS_{0.25}$), 0.125/0.50 (RF/VE-$TPGS_{0.50}$) and used as a pretreatment. Whereas specimens pre-treated with 0.125% riboflavin (RF) and those without any pre-treatment were considered as controls. For specimen preparation, the dentine specimens were etched for 15 s with 37% phosphoric acid (H_3PO_4) and thoroughly rinsed with distilled water for 5 min. The excess water was removed, and the dentine surface was left hydrated. Formulations were applied in one-application (10 μL) for 60 s, left undisturbed for 60 s, air-dried for 5 s, photo-activated with UVA ($\lambda = 368$ nm, output 7 mW/cm^2), and rinsed with distilled water. The UVA source used was placed 10 mm from the dentine surface with a spot

size of 7 mm, such that the whole dentine specimen was fully irradiated with a single UVA irradiation spot.

2.1. TEM investigation of dentine-collagen

TEM investigation was done to study structural variations of dentine collagen with the storage time in artificial-saliva (AS) modified with bacterial collagenase (Co) (100 U/mL) Type-I (AS/Co) as we previously have described [36]. In an occlusal-apical direction, vertical sections were made (1.0 mm) for each tooth as the exposed dentine surface was etched. After preparing a parallel cut to the occlusal surface, three dentine slabs (mid-coronal dentine) were obtained from each tooth. Dentine slabs ($n = 5$/*group*) were etched with 10 wt.% phosphoric acid for 5 h, cross-linked as previously described for experimental groups and then placed in the AS/Col at 37 °C for 1-week and 3 months. Later, slabs were fixed, buffered with 0.1 M sodium cacodylate for 1 h, treated by 1% osmium tetroxide (OsO_4) in phosphate buffered solution (PBS) for 1 h, rinsed with distilled water, dehydrated in ascending concentrations ethanol, and finally followed by infiltration with araldite resin. Ultra-microtome with a diamond knife was used to cut ultra-thin sections (~90 nm) from and collected on the grids and stained with uranyl-acetate, $UO_2(CH_3COO)_2{\cdot}2H_2O$, for 10 min before TEM imaging at 100 KV (JEOL-1010, Japan).

2.2. Micro-Raman analysis

All Raman spectroscopic experiments (n = 5/group) with dentine slabs prepared (demineralized and crosslinked as described previously for AFM and TEM) were carried out in a backscattering configuration using a triple monochromator (T-64000, Horiba/Jobin-Yvon, Kyoto, Japan) equipped with a charge coupled device (CCD) and polarization filters. The dentine specimens were dried with gentle stream of air at 35 °C for 15 min and the areas of ~10 μm were chosen randomly across all specimens. The excitation source for Raman scattering was on a focal spot of ~1.5 μm in diameter at zero calibration; with argon ion 514.5 nm laser (spectral resolution of 1.6 cm^{-1}) and power <500 μW at 100× objective with a superior signal/noise ratio and a near infra-red wave length to prevent thermal effects. The beam was focused through a water immersion objective (Nikon, Tokyo, Japan), through a notch filter (Kaiser Optical Systems), and imaged via a second lens identical to the first. A polynomial fitting routine with a non-negative peak constraint were removed to eradicate broad fluorescent backgrounds. All mathematical procedures were carried out with the aid of commercially available computational software (MATHEMATICA 7.0, Wolfram Research, Champaign, IL, USA). Now, the cross-linked specimens are substrates of considerable surface heterogeneity. This is why Raman spectra were recorded from 10 different random points of each specimen. The interpretation and results of presented show representative Raman peaks at room temperature. Baseline correction was performed by using polynomial fit to reduce the signal without losing information of small peaks and changing the peak ratio (Matlab; 200 iterations/5th order polynomial) [37]. The numbers were fit to avoid overfitting as the baseline did not cut through the original spectra that were taken to avoid losing data while recording mineralization on the cross-linked specimens. This baseline correction was standardized for all specimens.

2.3. Surface/bulk mechanical properties

Dentine beams, after crosslinking as previously described, were stored in AS/Col-solution at 37 °C for 24 h (baseline measurement) and 3 months and investigated for variations in surface/bulk mechanical properties. Nano-indentation testing was done at the desired time points. Testing was carried out with a G200 Nano-indenter (Agilent 7 Technologies, Santa Clara, CA, USA). The Berkovich diamond-indenter with a tip radius of 40 nm was used at a constant strain rate of 0.05 s^{-1} and a hold-time of 5 s at a maximum indentation depth of 70 nm at a load range of 400–500 μN. Fourteen indentations for each specimen (n = 7/group) were made on intertubular-dentine with a lateral spacing of 400 nm. The reduced elastic-modulus (E_r) and nano-hardness (H) were calculated. In addition, to investigate the effect of initial remineralization, on the mechanical properties and stability, demineralized and crosslinked (as described previously) dentine beams were tested after 14 days in artificial saliva, and AS/Co-solution after 24 h and 14 d respectively; moreover, after 14 days in the mineralization solution for the surface/bulk elastic modulus. Briefly, rectangular dentine beams of 0.5 × 1.7 × 6.5 mm were cut and demineralized in 10 wt.% phosphoric-acid for 5 h, rinsed in distilled water for 10 min and immediately cross-linked. Beams (n = 17/group) were fixed to a testing machine (5848 Microtester, Instron, Canton, MA, USA), and the load was applied at 0.5 mm/min crosshead-speed to 3% maximum strain [32].

2.4. Remineralization potential and AFM investigation

To investigate the effect of cross-linking on the initial remineralization potential of dentine collagen matrices, demineralized dentine slabs ($n = 5$) as prepared previously for TEM investigation, were crosslinked and placed in a mineralization solution. The mineralization solution was manufactured using 0.1 M $Ca(NO_3)_2$, 0.1 M $(NH_4)_2HPO_4$ to keep molar ratio of calcium/phosphorus to 1.67 and the concentration of calcium ions (Ca^{2+}) as10 mM, within the reaction system [38]. The pH was adjusted to 7.4 with 1 M NaOH and 0.1 M NH_4OH. Exposed mid coronal dentine surfaces were sequentially wet ground with 600–4000 grit-size silicon carbide papers (Carbimet, Buehler, Lake Bluff, IL, USA), polished with diamond paste (1.0 μm and 0.5 μm) on a rotary polishing machine (Buehler, Lake Bluff, IL, USA) and finally ultra-sonicated for 15 min in de-ionized water. Vertical sections were made in occlusal-apical direction of 2 mm depth dividing the dentine surface into 3 equal size specimens by a horizontal cut. After acid etching with 35% phosphoric-acid gel for 15 s, specimens were cross-linked as previously described for experimental groups, and specimens were stored in AS/Col for 14 days at 37 °C. The specimens were then placed in the mineralization solution at 37 °C for 24 h to be later investigated by AFM in tapping-mode (Multimode/AFM, NanoScope IV, Bruker Instruments, Singapore) using a silicon nitride probe (NP-S, Bruker) with a nominal tip radius of 10 nm at 18–24 KHz resonance frequency, and a 0.06–0.12 N/m spring constant. Some of dentine

specimens treated with RF/VE-TPGS$_{0.50}$ were mineralized and used for TEM investigation as described earlier in TEM section.

2.5. Collagenase-mediated degradation resistance (HYP-release)

The collagen content was determined using hydroxyproline assay [39] using an assay kit (BioVision, CA, USA) according to the manufacturer's instructions. Dentine slabs, with the dimensions of 4.5 mm length × 3.5 mm width × 0.5 mm thickness, were prepared from the coronal dentine and then demineralized in 10% phosphoric acid for 5 h. The demineralized slabs were rinsed and treated as described previously according to their respective groups ($n = 5$ dentin slabs/group). The specimens were exposed to 100 μg ml^{-1} of bacterial collagenase type 1 in tricine buffer for 24 h and 3 months respectively. Around 100 μl of supernatant was collected and hydrolyzed for 3 h in 12 M HCl at 120 °C. Next, 10 μl of aliquots from each group were transferred to a 96-well plate and dried under vacuum for evaporation. Later, 100 μl of Chloramine-T buffer reagent was added to the experimental and standard formulations and further incubated for 5 min at room temperature. In each well was later added 100 μl of DMAB reagent (DMAB and perchloric acid, $HClO_4$, 50 μl each) and incubated further at 60 °C for 90 min. Standard curves for the quantity of HYP (0–1 g/ml per well) [0–1gml–1/well] were generated using a spectrophotometer 96-well plate reader (Infinite 200 Tecan, Switzerland) at 560 nm absorbance. The hydroxyproline content for each specimen was averaged from quadruplicate measurements of each specimen.

2.6. Proteases expression detection

Specimens ($n = 10$) were prepared following a previous reported protocol by Daood et al. [40]. Teeth were sectioned using low speed diamond saw (Buehler, Lake Bluff, IL, USA) under water cooling and dentine beams from coronal part of the tooth were obtained. Dentin beams were prepared by removing the occlusal enamel and superficial dentin of each tooth with an Isomet saw (Buehler Ltd., Lake Bluff, IL, USA) under water cooling. A 1-mm thick mid-coronal dentin disk was prepared from each tooth. One dentine beam with dimensions 6 mm × 2 mm × 1 mm was then sectioned from the center of each disk. Beams for each group ($n = 20$/group) were demineralized using 10 wt.% phosphoric acid at 25 °C for 24 h, then rinsed using deionized water for 1 h. After cross-linking, they were analysed using ELISA (Human MMP2 ELISA; Human CTSK/Cathepsin-K., Lifespan Biosciences, Seattle, WA, USA).

2.7. Statistical analysis

Data were presented as mean ± standard deviation and analyzed by (SPSS v.15) analysis of variance (ANOVA), followed by the Tukey–Kramer *post hoc* test at a significance-level of $p \leq 0.05$. Data-normality was explored through test of normality table (Shapiro–Wilk and Kolmogorov–Smirnov tests) and normal Q–Q plots.

3. Results

3.1. TEM analysis

The structural degradation of dentine collagen network with storage in AS/Col solution for all groups is presented in the TEM images (Fig. 1). As a general pattern, all specimens showed varying degrees of structural changes after 3 months of storage compared with 1-week. However, the effect of the chemical enhancer (VE-TPGS) in preserving the integrity of dentine-collagen structure cross-linked with RF (Fig. 1F&H) can be clearly observed compared to the non-cross-linked (Fig. 1B) and RF-cross-linked (Fig. 1D) specimens without incorporation of VE-TPGS after 1-week and 3 months of storage. Evidence of structural degradation (Fig. 1A) with fairly identified characteristic collagen fibril structure with cross-banding was shown for negative control dentine specimens at 1-week. However, with 3-months storage of control specimens (Fig. 1B) there was absence of any organized collagen fibrillar lattice after the deterioration of collagen mesh and total loss of structure and periodicity which appear unidentifiably amorphous. Specimens treated with 0.125% RF showed preservation of well-formed collagen fibril structure with clear collagen cross-banding after 1-week storage. However, the collagen network exhibited a less dense structure with wider collagen interfibrillar spaces and shorter collagen fibrils. In contrary, after 3 months storage, RF crosslinked dentine-collagen without the VE-TPGS enhancer (Fig. 1C) showed clearer signs of structural degradation observed in terms of the formation of a less dense network structure, decreased collagen fibrils thickness and length, increased interfibrillar spaces, and sporadic evidence of gelatinous structure formation. Dentine specimens modified with 0.1% RF alone (Fig. 1D) with 1-week storage showing degradation of collagen network. Dentin specimens treated with RF modified with the permeation enhancer RF/VE-TPGS$_{0.25}$ (Fig. 1E) and RF/VE-TPGS$_{0.50}$ (Fig. 1G) showed an intact and dense collagen network with well-formed collagen fibrils having characteristic collagen cross-banding structure after 1 week storage. In addition, the collagen fibrils periodicity and gap/overlap zones are clearly visible by TEM after 3 months storage (Fig. 1G). After 3 months in AS/Col, specimens received the permeation enhancer (Fig. 1F&H) showed preservation of well-formed collagen fibril structure with clear collagen cross-banding, however, exhibited a less dense structure with wider collagen interfibrillar spaces and shorter collagen fibrils, especially with RF/VE-TPGS$_{0.25}$ (Fig. 1F) group. High magnification TEM imaging revealed the integrity in collagen fibrils structure and the uniformity in periodicity pattern after 3 months storage (Fig. 1I) of dentine specimens crosslinked with RF/VE-TPGS$_{0.50}$ (Fig. 1G). Periodicity of the collagen fibrils (indicators) reflected the precision in alignment of α1 and α2 chains of the collagen which preserved and maintained by extensive crosslinking.

3.2. Micro-Raman, bulk mechanical properties and AFM

The associated Raman analyses of dentine collagen from all groups are shown in (Figs. 2 B & 4 D–F). Raman spectra revealed

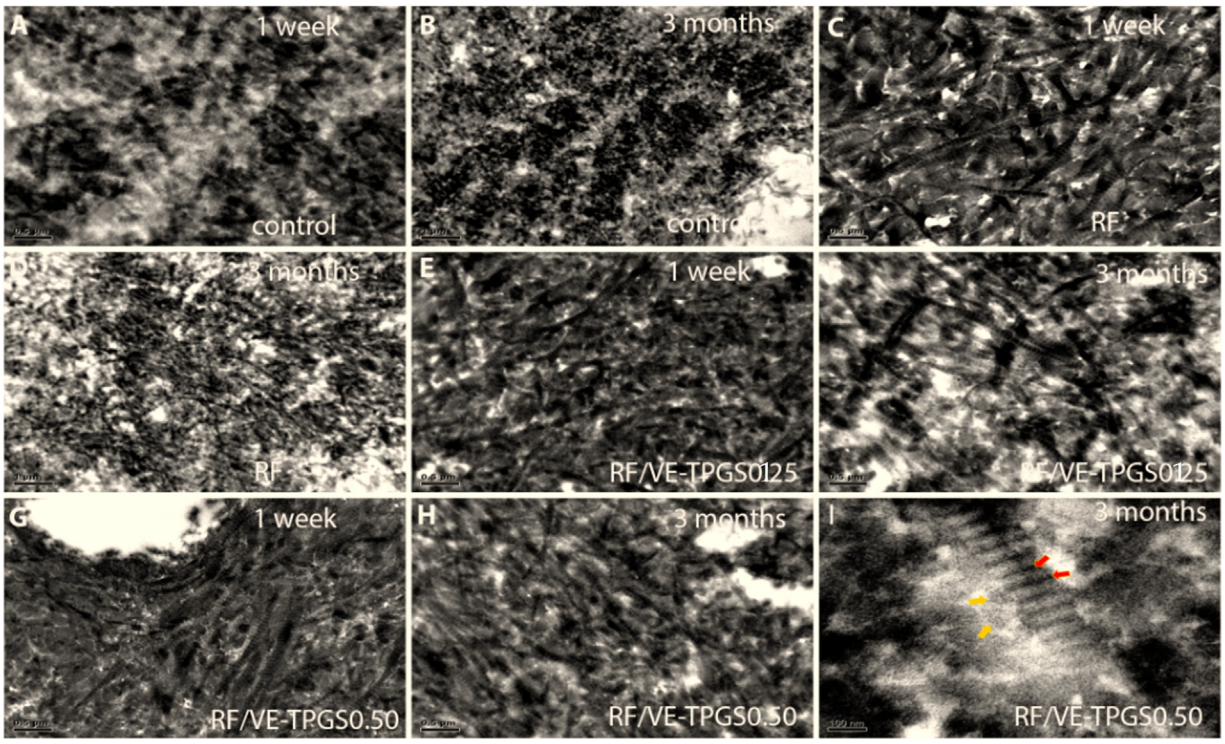

Fig. 1 – Selected transmission electron microscope (TEM) images showing the structure of dentine-collagen at 1 week and 3 months storage in artificial saliva modified with collagenase at 37 °C: (A) evidence of structural degradation with fairly identified characteristic collagen fibril structure with cross-banding was shown for negative control dentine specimens at 1 week. (B) 3-months storage of control specimens showing absence of any organized collagen fibrillar lattice. (C) Specimens treated with RF showed preservation of well-formed collagen fibril structure with clear collagen cross-banding after 1-week storage. (D) After 3 months storage, RF crosslinked dentine-collagen without the VE-TPGS enhancer showed clearer signs of structural degradation. (E) Dentine specimens modified with RF/VE-TPGS0.125% alone with one-week storage showing degradation of collagen network. (F) Dentine specimens treated with RF/VE-TPGS$_{0.125}$ after 3 months of storage; (G) RF/VE-TPGS$_{0.50}$ showed an intact and dense collagen network with well-formed collagen fibrils having characteristic collagen cross-banding structure after 1 week storage. (H) After 3 months in artificial saliva/collagenase, specimens received the permeation enhancer RF/VE-TPGS$_{0.50}$ showed preservation of well-formed collagen fibril structure. (I) High magnification TEM imaging revealed the integrity in collagen fibrils structure and the uniformity in periodicity pattern after 3 months storage crosslinked with RF/VE-TPGS$_{0.50}$. The yellow arrows indicated apatite crystallites aligned along the collagen axis after mineralization. The red arrows indicated overlap collagen band zones identified in the fibril. Presence of apatite complexes along the the fibril's surface in the intrafibrillar spaces (yellow arrowheads) supports the mineralization potential after true crosslinking. (For interpretation of the references to color in this figure legend, the reader is referred to the web version of this article.)

the structural integrity and conformational stability of collagen fibrils cross-linked with RF/VE-TPGS, compared to the other groups. Raman data showed the details of chemical interactions between the crosslinking formulations and demineralized dentine collagen before (Fig. 2B) and after (Fig. 4D–F) remineralization. Banding analysis of demineralized control and crosslinked dentine matrices showing (Fig. 2A) high magnification TEM images showing collagen fibril axial periodicity banding; and (Fig. 2B) the associated Raman analysis. The Amide I band is centered at 1655 cm^{-1} arising from C=O stretching of the peptidic bond in the Gly-X-Y tripeptide sequence. The frequency shift is a clear indication of a different proportion of amino acid residues within the X and Y positions within the collagen structure (representative of the α-helix structure). The specimens of RF/VE-TPGS$_{0.50}$ modified dentine collagen had distinct overlap zones showing a highly polarized state. The RF/VE-TPGS$_{0.50}$ and RF/VE-TPGS$_{0.25}$ averaged almost identical Raman bands. The positions of N- and C-telopeptides are shown as blue lines labelled with N and C between gap and overlap zones which preclude alignment of the collagen profile determining orientation of the collagen fiber amicably modified with crosslinkers within 1595 cm^{-1} and 1655 cm^{-1} zone. The positions of X1, X2 and X3 (shown with red lines), the three major ridges relative to collagen gap zones correlate to the modification with crosslinkers again orienting the collagen fiber within the dentine as the relative peaks for chemical enhancer groups occur at much higher intensities. These intensities were identified as the nearest neighbor to the Amide I band region and thus were able to orient the collagen profile. Although the bands (X1, X2 and X3) are similar among the different specimens, some differences appeared in the minor bands. Differences in the peak periods

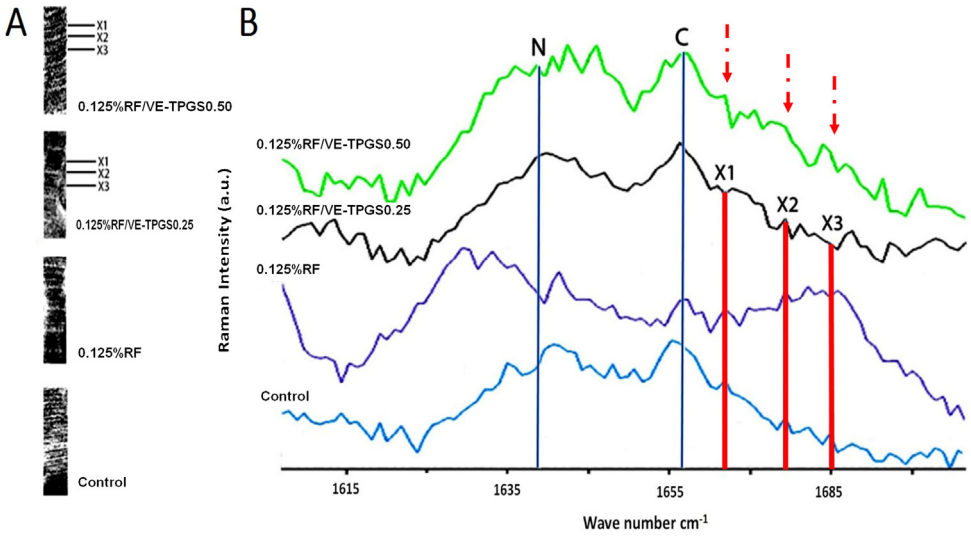

Fig. 2 – (A) Banding analysis of demineralized control and crosslinked dentine matrices showing high magnification TEM images showing collagen fibril axial periodicity banding; and (B) the associated Raman analysis. The positions of N- and C-telopeptides are shown as blue lines labelled with N and C between gap and overlap zones which preclude alignment of the collagen profile determining orientation of the collagen fiber amicably modified with crosslinkers within 1595 cm^{-1} and 1655 cm^{-1} zone. The positions of X1, X2 and X3 (shown with red lines), the three major ridges relative to collagen gap zones correlate to the modification with crosslinkers again orienting the collagen fiber within the dentine as the relative peaks for chemical enhancer groups occur at much higher intensities. (For interpretation of the references to color in this figure legend, the reader is referred to the web version of this article.)

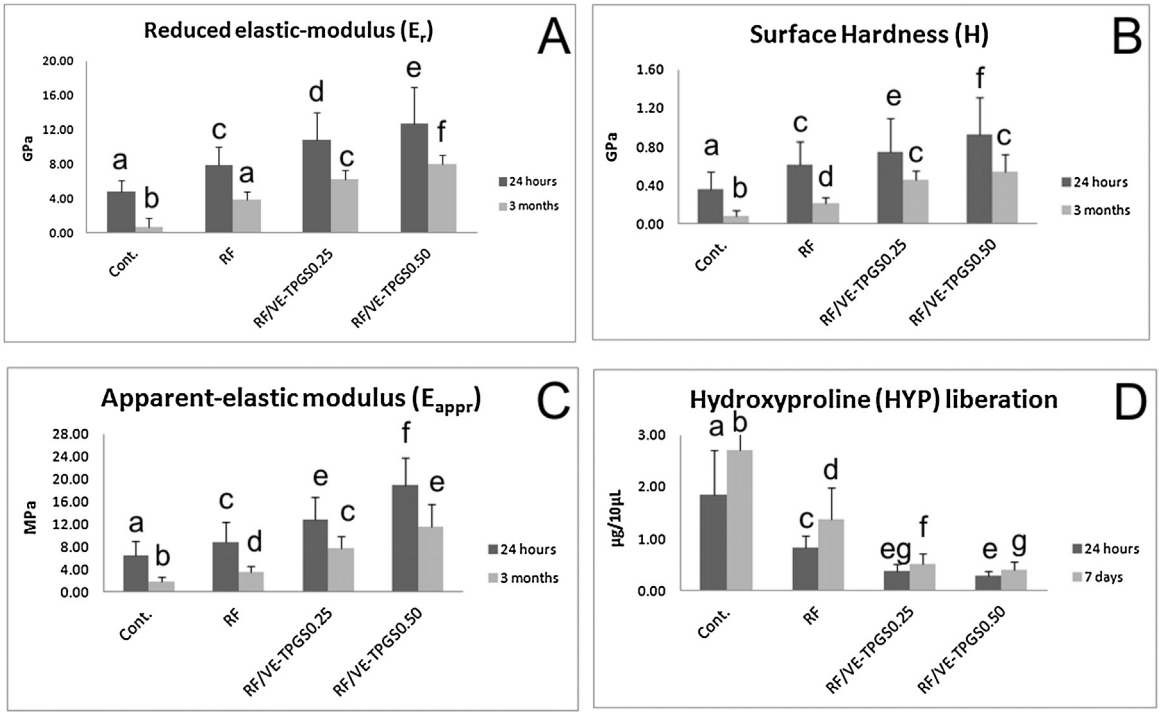

Fig. 3 – Means ± standard deviations of the variations in the surface mechanical properties (nano-indentation) in terms of: (A) reduced elastic modulus (E_r) and hardness; (B): (H) with storage in artificial saliva (AS) modified with collagenase type I (AS/Col) solution for 24 h and 3 months. Means ± standard deviations of the variations in the apparent bulk elastic modulus (E_{appr}) with the storage in AS modified with collagenase type I (AS/Col) solution for 24 h and 3 months; (C): Means ± standard deviations of the hydroxyproline (HYP) release after 24 h and 7 days exposure to collagenase type I solution. (D): Bars with different lowercase letters are statistically significant at $P \leq 0.05$.

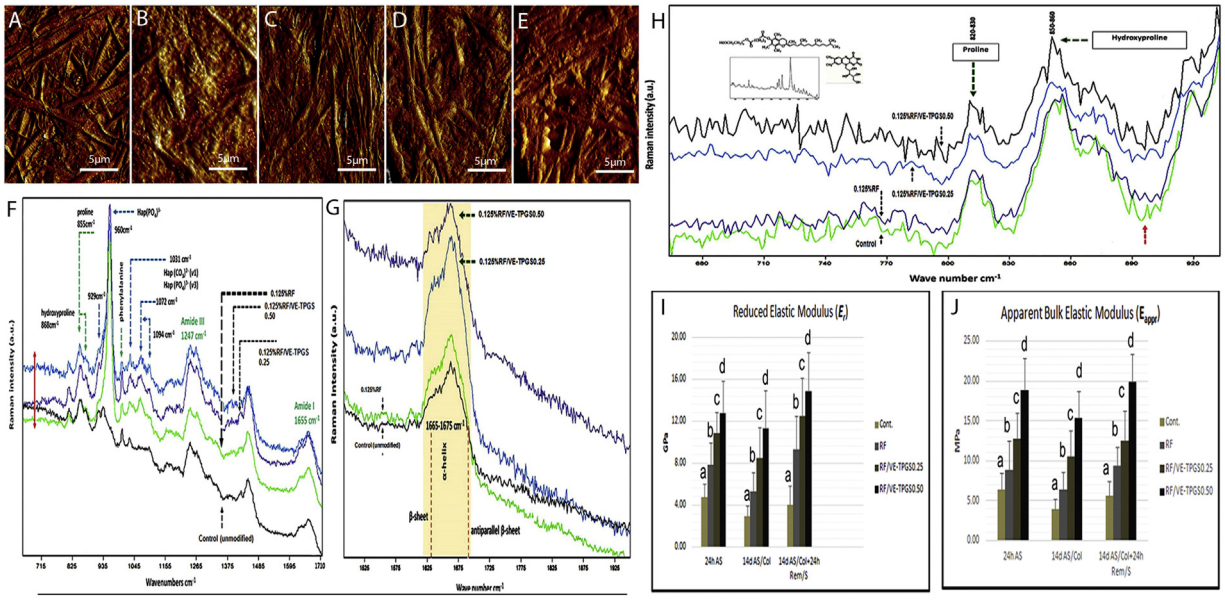

Fig. 4 – (A) AFM amplitude images of demineralized dentine specimens crosslinked with RF/VE-TPGS$_{0.50}$ showing the high integrity of collagen fibrils. The structural integrity of non-mineralized collagen fibers can be seen with the periodic stripes. (B) AFM image of dentine specimens after 24 h mineralization, without collagen crosslinking modification showing minimal amount of mineral deposits depicting an irregular rough surface; (C) dentine specimens after 24 h mineralization under RF crosslinking. The lower crosslinking degree of collagen fibers enables the morphology of collagen fiber after mineralization to be still seen. After 24 h in the mineralization solution, AFM images revealed the clear minerals formation in close association with/on the collagen fibrils obliterating the characteristic cross-banding and interfibrillar spaces which was more prominent with specimens crosslinked with (D) RF/VE-TPGS$_{0.25}$; and RF/VE-TPGS$_{0.50}$ (E). With the increase of collagen crosslinking with permeation enhancers, more and more minerals are seen attached on the surface of collagen. Since we source the apatite from the mineralization process, the content of minerals can directly be quantitatively reflected by the Raman method. Raman spectra after 24 h in the mineralization solution at different spectral ranges are presented in figures (F–H). (F) The red arrow represents the intensities in accordance to the intensity of crosslinking amongst all groups. (G) The intensities are also well visualized in specimens, especially crosslinked with RF/VE-TPGS$_{0.25}$; and RF/VE-TPGS$_{0.50}$. (H) The inset Raman (boxed at the left side) represents the riboflavin representative peaks. The intensity represents the sharp shoulders of the hydroxyproline peak which also represents the intensities in accordance to the intensity of crosslinking amongst all groups. (I) Means ± standard of the reduced elastic-modulus (E_r) and the apparent bulk elastic-modulus (E_{appr}) (J) with the storage in the AS/Col solution for 24 h and 14 days; and after 24 h in the mineralization solution. Bars with different lowercase letters, within each storage condition, are statistically significant at $P \leq 0.05$.

are apparent, but the consistency between different periods may not be good enough to allow reliable comparison.

Significant differences in the surface/bulk mechanical properties were found within each group between both time points, namely 1-week and 3 months in the AS/Col (Fig. 3A–C). However, crosslinking with RF/VE-TPGS consistently showed significantly higher surface/bulk mechanical-properties especially with the increase in VE-TPGS content. The same trend was also recorded for the HYP-liberation (Fig. 3D) reflecting the higher collagenase-mediated degradation resistance with RF/VE-TPGS formulations. In contrary, non-cross-linked group showed the least mechanical and chemical stabilities.

This observation is also confirmed by the AFM study (Fig. 4A), reflecting the precision in the alignment of α1- and α2-chains of collagen through the efficient cross-linking using photo-activated RF coupled with VE-TPGS. Which is, on the other hand, indicating high conformational stability especially at higher VE-TPGS content. This was generally observed in all specimens analyzed for the purpose. AFM images (Fig. 4A) confirmed the high integrity of collagen fibrils with the characteristic collagen cross-banding structure of demineralized specimens cross-linked with RF/VE-TPGS$_{0.50}$. In addition, after 24 h in the mineralization-solution, AFM images revealed clear minerals formation in close association with the collagen-fibrils obliterating the characteristic cross-banding and interfibrillous spaces which was more prominent with specimens' cross-linked with RF/VE-TPGS (Fig. 4D&E). AFM amplitude images of (Fig. 4A) demineralized dentine specimens crosslinked with RF/VE-TPGS$_{0.50}$ showing the high integrity of collagen fibrils with the characteristic collagen cross-banding structure. After 24 h in the mineralization solution, AFM images revealed the clear minerals formation in close association with/on the collagen fibrils obliterating the characteristic cross-banding and interfibrillar spaces which was more prominent with specimens crosslinked with (Fig. 4D) RF/VE-TPGS$_{0.25}$; and RF/VE-TPGS$_{0.50}$

Table 1 – Expression of MMP-2 and Cathepsin K activities (ng/ml) obtained with Human MMP-2 and Cathepsin- K ELISA Kit system.

Groups	MMP-2	Cathepsin-K
Control	19.1 ± 3.2^{A}	4.6 ± 2.2^{A}
1% Rf	11.8 ± 2.4^{B}	1.2 ± 0.81^{B}
RF/VE-TPGS$_{0.25}$	3.33 ± 1.7^{C}	0.71 ± 0.33^{C}
RF/VE-TPGS$_{0.50}$	1.76 ± 0.91^{D}	0.103 ± 0.05^{D}

Uppercase letters represent differences in each column ($P \leq 0.05$).

(Fig. 4E). The Raman analysis (Fig. 4F) confirmed the band assignments associated with inorganic phase (HAp) seen as peaks at 960, 1031, 1072 and 1094 cm^{-1} which appear with increased intensities as the content of VE-TPGS increases. Furthermore, the amide and HYP related bands exhibited changes within the groups with bands increasing in intensity for RF/VE-TPGS$_{0.50}$ treated group (Fig. 4F–G). In Fig. 4H, it was reasonable to assume the configuration of hydroxyproline within the spectral result of collagen fibrils. It was interesting to note that the relative intensity of the hydroxyproline/proline bands, normalized at 850–860 and 820–830 cm^{-1}, increased with increasing in chemical enhancer content after mineralization. This increase in intensity for the spectrum is because of the hydroxyproline with spectra for control and RF-crosslinked specimens slightly altered and having decreased intensities. The red arrow represents the sharp shoulder of the hydroxyproline peak which also represents the intensities in accordance to the intensity of crosslinking amongst all groups. the inset Raman (boxed at the left side) represents the riboflavin representative peaks. The chemical enhancer containing formulations, also, resulted in an increase in the CN-band intensity and a decrease in the NH-plane.

Significant improvement in surface/bulk elastic modulus was found after 24 h in the mineralization solution confirming the higher initial remineralization potential of collagen fibrils cross-linked with RF/VE-TPGS (Fig. 4I&J). Means ± standard of the reduced elastic-modulus (E_r) (Fig. 4I) and the apparent bulk elastic-modulus (E_{appr}) (Fig. 4J) with the storage in the AS/Col solution for 24 h and 14 days; and after 24 h in the mineralization solution. Bars with different lowercase letters, within each storage condition, are statistically significant at $P \leq 0.05$.

3.3. *Protease expression*

The results of MMP-2 and cathepsin-K activities are shown (Table 1). The concentrations and expression of active enzymes present in the non-cross-linked and RF-cross-linked groups were significantly higher than the two groups cross-linked with RF/VE-TPGS. However, there was a significant decrease in proteases activities with the increase in the VE-TPGS content.

4. Discussion

The objective of this laboratory study was to investigate dentine collagen cross-linking when this procedure is synergized with different concentrations of a riboflavin permeation enhancers. That said, some new formulations have been defined and modified from previous protocols of corneal collagen [23] and dentine collagen [30,31] crosslinking combining D-Alpha-tocopheryl-poly(ethylene-glycol), as a crosslinking enhancer with UVA-activated riboflavin. Riboflavin forms a defensive-shield against possible UVA absorption producing proteoglycan-core proteins and collagen crosslinking bond [41]. However, high viscosity molecular weight molecules may have a limiting effect on the further penetration of RF within extracellular-matrices [34]. Starting from these evidences, the potential significance of VE-TPGS in enhancing the RF permeation and accumulation by dentine collagenous-based protein matrices and the subsequent crosslinking efficiency was investigated.

Based on the results of the current study that showed the significant synergetic effect of VE-TPGS when combined with UVA-activated RF, all null-hypotheses tested should be rejected. In addition, this synergetic effect is positively dependent on the VE-TPGS content. Such improvement in demineralized dentin-collagen crosslinking efficiency reflected by higher structural integrity and conformational-stability of dentine-collagen fibrils shown by TEM (Fig. 1), superior mechanical-stability (Fig. 3A–C), improvement in collagenase-mediated resistance to degradation (Fig. 3D) and lower endogenous proteases expressions (Table 1) might be attributed to higher riboflavin permeation and uptake by dentine collagenous-matrices, as there were previous reports of RF uptake in collagen fibers inside corneal-collagen [28]. In should be noted that the crosslinking formulations and technique used in this study employed relatively low RF-solution concentration (0.125%) and 60 s application of time to avoid unwanted side effects such as dentine discoloration.

TEM investigations (Fig. 1) revealed more closed and integer demineralized collagen network structure; and denser interfibrillous spaces supporting the significance effect of using RE/VE-TPGS after 1-week and 3 months in AS/Col solution. In addition, collagen fibrils showed well-demarcated collagen cross-banding pattern (Figs. 1 and 2) which could be attributed to changes in orientation of tropocollagen molecules, leading to denser dentine collagen matrix [42]. Such aggregation was increased and intensified with increasing with the VE-TPGS content. Moreover, the conformational heterogeneity of collagen appeared due to increased cross-linking as also confirmed with micro-Raman analysis (Fig. 2). The banded structure observed in TEM (Fig. 1I) and AFM (Fig. 4A) imaging, especially with RF/VE-TPGS$_{0.50}$, indicates an array of gap/overlap zones in a stable normal collagen structure. This is showing parallel arrangement which is a part of close bundles with clearly visible alternate light and dark bands. Moreover, profile-analysis of dentine-collagen exhibits same major features within all experimental groups with internal consistency between different periods noted. Averaged images of collagen fibrils in RF/VE-TPGS groups suggested similar banding patterns probably referring to collagen periodicity at 69.0 nm and 65.6 nm. This was very clear specially for RF/VE-TPGS$_{0.50}$ which are in accordance to collagen periodicity in other tissues [43]. However, there is a suspected change in D-spacing of cross-linked collagen fibrils compared to mineralized fibrils as the collagen structure presumably relaxes within its non-mineralized D-spacing after demineralization [44]. After micro-Raman band-profiling (Fig. 2), increased intensities termed as X1/X2

(Fig. 2B) with RF/VE-TPGS formulations, could be due to protein backbone residues within the collagen fibrils [45]. The addition of RF/VE-TPGS to cross-linking formulation enhanced X1/X2 intensities as they represented increased density from N- and C-termini-axially contracted telopeptide domains [46]. That said, the X3 band exhibited high observable intensity in the experimental study groups which was possibly due to compact confirmation of an axial helical terminus.

The banding-pattern, again, might be explained by the changes in orientation of the tropocollagen molecules, with respect to fibril long-axis or in secondary tertiary-structure of collagen. The tocopherol is bound to have an open conformation with a sealed hydrophobic component [47] which attaches to highly mobile collagen fragment [48] and maintains the helical structure. The vitamin E present within the formulation might also act as a scavenger of superoxides and stabilizes cellular membranes [49]. Although VE-TPGS facilitates formation of micelles and could be useful for lipid drug delivery systems, vitamin E may be present and penetrate within dentine because dentinal fluid and dentine can act as peroxide and oxygen reservoirs [50], which are present at the collagen surface. Thus, VE-TPGS, may be indicated in an endeavour to neutralize the free oxygen present in a higher amount in dentine after riboflavin free radical formation.

The changes observed in the micro-Raman peak positions and relative intensities for collagen changes suggested that an interaction took place at the functional group relative for collagen cross-linking. The results were consistent with the mineralization studies: a shift and broadened peak corresponding to the TPGS (C=O) stretching vibration [51] is usually observed at 1730 cm^{-1}, indicating a hydrogen bonding interaction. But this was not observed among the micro-Raman peaks, also indicating no degradation products of the compound.

The lower expression of proteases after crosslinking additionally reflected the synergetic effects of the experimental crosslinking formulations (Table 1). The expression of MMP-2 and Cathepsin-K was significantly reduced in RF/VE-TPGS groups with lowest levels seen in RF/VE-$TPGS_{0.50}$ ($P < 0.05$). Authors conclude that the release of reactive-oxygen species on collagen fibrils may have induced breakdown of weak intrinsic crosslinks and formed covalent cross-links instead via UVA oxidation pathway. Excessive cross-linking may have altered or disabled active enzymes configuration sites, making them unable to accept a complementary peptide-sequence which further would be blocking and inhibiting their proteolytic activities. This may have hydrolyzed specific peptide bonds, preserving integrity and tethering telopeptides to collagen by pyridinium cross-links [52].

The mechanical stability with challenges in collagenase containing AS could be considered an indirect evaluation of riboflavin crosslinking effect. Characterization of bulk modulus only could give indication on the penetrative effect of the cross-linking formulations on mechanical stability of dentine collagen matrices. The improvement in surface/bulk mechanical stability (Fig. 3A–C) of demineralized dentine specimens with RF/VE-TPGS should be considered as a further confirmation of such a synergetic effect and explain as previous. The released HYP is due to the action of bacterial-collagenase and other dentine-bound proteases [53]. Although a HYP-assay is non-specific, however, it might give indication of tissue collagen concentration. The lower HYP liberation (Fig. 3D) found with RF/VE-TPGS cross-linked groups could reflect the higher collagen content and the superior biodegradation resistance against the collagenase effect. Moreover, the oxidation product of tocopherol are tocopheroxyl radicals, produced by peroxyl radicals. These compounds are readily hydrolyzed in acidic conditions and reduced reversibly [54].

Cross-linking could affect the mineralization potential by providing and maintaining collagen fibrils' structural, chemical and mechanical integrity [41]. In addition, collagen fibrils exhibit the ability to align more due to an increase in the mineral fraction [55]. Therefore, the control and experimental dentine collagen matrices were placed in a mineralizing-solution for 24 h to study the initial remineralization potential by AFM coupled with micro-Raman analysis (Fig. 4). AFM images show considerable mineral depositions in close association with dentine collagen fibrils and at the interfibrillous spaces especially with RF/VE-TPGS formulations (Fig. 4D&E) after 24 h in the mineralization-solution. In addition, the micro-Raman data showed the molecular band assignments associated with the inorganic phase (HAp) seen at 960 cm^{-1}, 1031 cm^{-1}, 1072 cm^{-1} and 1094 cm^{-1} – which appear with increased intensities as the concentration of VE-TPGS increases supporting the interpretation of the AFM results (Fig. 4F). In addition, there is an increase in amide I (Fig. 4G) and III (Fig. 4H) bands, also indicative of increased collagen alignment. It was suggested that amide I and III vary and are sensitive to hydrogen bonding pattern changes within the collagen structure [56,57]. If this explanation is deemed correct, changes within amino acid chains along polypeptide-chains after cross-linking would manifest themselves within the Raman spectra. Our results comparing amide III and amide I after cross-linking with RF/VE-TPGS formulations, show a difference which is apparent between the cross-linked and control groups. This could be suggesting that collagen is different from that in the control collagen matrices and is also more aligned and structured. This, on the other hand, would be presumably supporting the assumption that dentine-collagen matrix is forming an altered, more aligned, extracellular matrix to support mineralization with cross-linking. Fig. 4F shows dominant hydroxyproline band normalized to the proline-band at 855 cm^{-1}. It is very interesting to note that the relative intensity of the hydroxyproline band has increased within specimens treated with RF/VE-TPGS formulations. These are same specimens that had also showed increased minerals formation. Given this, high hydroxyproline intensity groups would have affected hydrogen banding pattern and collagen secondary structure. The presence of hydroxyl groups can affect physiochemical environment of collagen fibrils [58] and this would create sites for nucleation and growth for hydroxyapatite crystals [59]. Collagen structure changes manifested within amide I bands have long been used in Raman spectroscopy as indirect measure of collagen cross-linking. Calculated hydroxyproline bands, corresponding to the ring breathing modes, are useful in the interpretation of analysis of vibrational spectral modes.

A mineralised phase associated with collagen fibrils account for its strength and toughness due to more effec-

tive load-transfer within dentine [60]. Salt bridges are formed between mineral crystals and collagen, providing an eff ; ;ective load transfer mechanism between the mineral and organic phases that also enhances energy dissipation to minimize stress formation [61]. Mineralized collagen-matrices have the tendency to produce higher levels of lysylpyridinoline mature crosslinks compared to nonmineralized collagen-matrices. The non-mineralized collagen matrices show an abundance of hydroxylysylpyridinoline links [62]. Furthermore, the axial compression and lateral expansion of collagen fibrils, because of possible mineralization, could also serve as a mechanism for resultant strength [45]. In addition to the more efficient collagen crosslinking, the previous could explain the higher mechanical-properties reported with RF/VE-TPGS treated dentine matrices after 24 h in the mineralization solution (Fig. 4G&H). The mineralization process occurs due to nucleation of hydroxyapatite crystals inside the halo zones of collagen stored between the tropo-collagen molecules [63]. Type I collagen by itself cannot induce apatite nucleation [64], therefore synthetic agents (crosslinking agents) can be used to improve mechanical properties. The induced mineralization itself may influence the pyridinoline and deoxypyridinoline crosslinks [65].

Formulations containing permeation enhancers could be of significant potential in facilitating penetration, distribution and uptake riboflavin, a hydrophilic salt of lipophilic nature, through extracellular and collagen matrices [66]. TPGS displays significant surface activity and can solubilize a variety of water soluble compounds being stable at 4.5–7.5 pH [67]. The use of VE-TPGS as a synergistic material in the synthesis of a novel crosslinking formulation and its cytotoxic effects alone or by a combination with RF remains to be addressed. The current laboratory study showed that VE-TPGS might be an effective enhancer of UVA-activated riboflavin effect on dentine collagen matrices for potential application in dentine bonding. Moreover, VE-TPGS is effective in quenching harmful reactive-oxygen species [25]. This might favor the polymerization of adhesive-monomers, however, this will be investigated in details later.

5. Conclusion

The results showed a significant synergetic effect of VE-TPGS when combined with riboflavin. It could be concluded that the synergetic effect of VE-TPGS potentializes the riboflavin as cross-linking agent, improving the conformational stability and mechanical properties, reducing the enzymatic degradation and inducing the remineralization process.

Acknowledgments

This work was supported by the Ministry of Education, Singapore; ARF/NUS R221000039133. The authors thank International Medical University and Nanocat University of Malaya for their assistance in Raman work.

REFERENCES

[1] Tabatabaei FS, Tatari S, Samadi R, Moharamzadeh K. Different methods of dentine processing for application in bone tissue engineering: a systematic review. J Biomed Mater Res A 2016;10:2616–27.
[2] Tjäderhane L, Nascimento FD, Breschi L, Mazzoni A, Tersariol IL, Geraldeli S. Optimizing dentin bond durability: control of collagen degradation by matrix metalloproteinases and cysteine cathepsins. Dent Mater 2013;29:116–35.
[3] Tjäderhane L, Nascimento FD, Breschi L, Mazzoni A, Tersariol IL, Geraldeli S. Strategies to prevent hydrolytic degradation of the hybrid layer — a review. Dent Mater 2013;29:999–1110.
[4] Mazzoni A, Pashley DH, Nishitani Y, Breschi L, Mannello F, Tjäderhane L. Reactivation of inactivated endogenous proteolytic activities in phosphoric acid-etched dentine by etch-and-rinse adhesives. Biomaterials 2006;27: 4470–6.
[5] Aguda AH, Panwar P, Du X, Nguyen NT, Brayer GD, Brömme D. Structural basis of collagen fiber degradation by cathepsin K. Proc Natl Acad Sci U S A 2014;49:17474–9.
[6] Ferrari M, Mason PN, Goracci C, Pashley DH, Tay FR. Collagen degradation in endodontically treated teeth after clinical function. J Dent Res 2004;83:414–9.
[7] Frassetto A, Breschi L, Turco G, Marchesi G, Di Lenarda R, Tay FR. Mechanisms of degradation of the hybrid layer in adhesive dentistry and therapeutic agents to improve bond durability — a literature review. Dent Mater 2016;32:e41–53.
[8] Tjäderhane L, Nascimento FD, Breschi L, Mazzoni A, Tersariol IL, Geraldeli S. Optimizing dentin bond durability: control of collagen degradation by matrix metalloproteinases and cysteine cathepsins. Dent Mater 2013;29:116–35.
[9] Sabatini C, Pashley DH. Mechanisms regulating the degradation of dentin matrices by endogenous dentin proteases and their role in dental adhesion. A review. Am J Dent 2014;27:203–14.
[10] Yang B, Adelung R, Ludwig K, Bossmann K, Pashley DH, Kern M. Effect of structural change of collagen fibrils on the durability of dentin bonding. Biomaterials 2005;26:5021–31.
[11] Carrilho MR, Geraldeli S, Tay F, de Goes MF, Carvalho RM, Tjäderhane L, et al. In vivo preservation of the hybrid layer by chlorhexidine. J Dent Res 2007;86:529–33.
[12] Sano H, Takatsu T, Ciucchi B, Horner JA, Matthews WG, Pashley DH. Nanoleakage leakage within the hybrid layer. Oper Dent 1995;20:18–25.
[13] Ferracane JL. Hygroscopic and hydrolytic effects in dental polymer networks. Dent Mater 2006;22:211–22.
[14] Pashley DH, Tay FR. Collagen degradation by host-derived enzymes during aging. J Dent Res 2004;83:216–21.
[15] Chung L, Dinakarpandian D, Yoshida N, Lauer-Fields JL, Fields GB, Visse R, et al. Collagenase unwinds triple-helical collagen prior to peptide bond hydrolysis. EMBO J 2004;23:3020–30.
[16] Chiang YS, Chen YL, Chuang SF, Wu CM, Wei PJ, Han CF, et al. Riboflavin-ultraviolet-A-induced collagen cross-linking treatments in improving dentin bonding. Dent Mater 2013;6:682–92.
[17] Zhang Z, Mutluay M, Tezvergil-Mutluay A, Tay FR, Pashley DH, Arola D, et al. Effects of EDC crosslinking on the stiffness of dentin hybrid layers evaluated by nanoDMA over time. Dent Mater 2017;8:904–14.
[18] Gendron R, Grenier D, Sorsa T. Inhibition of the activities of matrix metalloproteinases 2, 8, and 9 by chlorhexidine. Clin Diagn Lab Immuno 1999;6:437–9.

[19] Scaffa PM, Vidal CM, Barros N, Gesteira TF, Carmona AK, Breschi L, et al. Chlorhexidine inhibits the activity of dental cysteine cathepsins. J Dent Res 2012;91:420–5.
[20] Tezvergil-Mutluay A, Agee KA, Uchiyama T, Imazato S, Mutluay MM, Cadenaro M, et al. The inhibitory effects of quaternary ammonium methacrylates on soluble and matrix-bound MMPs. J Dent Res 2011;90:535–40.
[21] Tezvergil-Mutluay A, Mutluay M, Gu L, Zhang K, Agee KA, Carvalho RM. The anti-MMP activity of benzalkonium chloride. J Dent 2011;39:57–64.
[22] Xie Q, Bedran-Russo AK, Wu CD. In vitro remineralization effects of grape seed extract on artificial root caries. J Dent 2008;36:900–6.
[23] Wollensak G, Aurich H, Wirbelauer C. Potential use of riboflavin/UVA cross-linking in bullous keratopathy. Ophthalmic Res 2008;41:114–7.
[24] Mohanty B, Mishra SK, Majumdar DK. Effect of formulation factors on in vitro transcorneal permeation of voriconazole from aqueous drops. J Adv Pharm Technol Res 2013;4:210–6.
[25] Leccisotti A, Islam T. Transepithelial corneal collagen cross-linking in keratoconus. J Refract Surg 2010;12:942–8.
[26] Stojanovic A, Zhou W, Utheim TP. Corneal collagen cross-linking with and without epithelial removal: a contralateral study with 0.5% hypotonic riboflavin Solution. BioMed Res Int 2014;619398:9.
[27] Caruso C, Ostacolo C, Epstein RL, Barbaro G, Troisi S, Capobianco D. Transepithelial corneal cross-linking with vitamin E-enhanced riboflavin solution and abbreviated, low dose UV-A: 24-month clinical outcomes. Cornea 2016;2:145–50.
[28] Osracolo C, Caruso C, Tronino D, Troisi S, Laneri S, Pacente L, et al. Enhancement of corneal permeation of riboflavin-5′-phosphate through vitamin E TPGS: a promising approach in corneal trans-epithelial cross linking treatment. Int J Pharm 2013;2:148–53.
[29] Constantinides PP, Han J, Davis SS. Advances in the use of tocols as drug delivery vehicles. Pharm Res 2006;23:243–55.
[30] Bharat Mehta A, Kumari V, Jose R, Izadikhah V. Remineralization potential of bioactive glass and casein phosphopeptide-amorphous calcium phosphate on initial carious lesion: an in-vitro pH-cycling study. J Conserv Dent 2014;1:3–7.
[31] Kim YK, Yiu CK, Kim JR, Gu L, Kim SK, Weller RN, et al. Failure of a glass ionomer to remineralise apatite-depleted dentin. J Dent Res 2010;89:230–5.
[32] Fawzy AS, Nitisusanta L, Iqbal K, Umer D, Beng LT, Neo J. Characterization of riboflavin-modified dentin collagen matrix. J Dent Res 2012;11:1049–54.
[33] Cova A, Breschi L, Nato F, Ruggeri A, Carrilho M, Tjäderhane L, et al. Effect of UVA-activated riboflavin on dentin bonding. J Dent Res 2011;12:1439–45.
[34] Hass V, Luque-Martinez IV, Gutierrez MF, Moreira CG, Gotti VB, Feitosa VP, et al. Collagen cross-linkers on dentin bonding: stability of the adhesive interfaces, degree of conversion of the adhesive, cytotoxicity and in situ MMP inhibition. Dent Mater 2016;6:732–41.
[35] Ostacolo C, Caruso C, Tronino D, Troisi S, Laneri S, Del Prete A, et al. Enhancement of corneal permeation of riboflavin-5'-phosphate through vitamin E TPGS: a promising approach in corneal trans-epithelial crosslinking treatment. Int J Pharm 2013;2:148–53.
[36] Priyadarshini BM, Lu TB, Fawzy AS. Effect of photoactivated riboflavin on the biodegradation-resistance of root-dentin collagen. J Photochem Photobiol B 2017;177:18–23.
[37] Lieber CA, Mahadevan-Jansen A. Automated method for subtraction of fluorescence from biological Raman spectra. Appl Spectrosc 2003;11:1363–7.
[38] Du T, Niu X, Li Z, Li P, Feng Q, Fan Y. Crosslinking induces high mineralization of apatite minerals on collagen fibers. Int J Bio Macromol 2018;1:450–7.
[39] Zeugolis D, Paul R, Attenborough G. Factors influencing the properties of reconstituted collagen fibers prior to self-assembly: animal species and collagen extraction method. J Biomed Mater Res A 2008;86:892–904.
[40] Daood U, Yiu CK, Burrow MF, Niu LN, Tay FR. Effect of a novel quaternary ammonium silane on dentin protease activities. J Dent 2017;3:19–27.
[41] Hayes S, Kamma-Lorger CS, Boote C. The effect of riboflavin/UVA collagen cross-linking therapy on the structure and hydrodynamic behaviour of the ungulate and rabbit corneal stroma. PLoS One 2013;8:e52860.
[42] Ortolani F, Marchini M. GA banding: a new terminology and a study of the glutraldehyde induced band pattern of type I collagen fibrils. Boll Soc Ital Biol Sper 1993;69:49–55.
[43] Orgel JPRO, Irving TC, Miller A, Wess TJ. Microfibrillar structure of type I collagen in situ. Proc Natl Acad Sci U S A 2006;103:9001–5.
[44] Karunaratne A, Esapa CR, Hiller J, Boyde A, Head R, Bassett JH, et al. Significant deterioration in nanomechanical quality occurs through incomplete extrafibrillar mineralization in rachitic bone: evidence from in-situ synchrotron X-ray scattering and backscattered electron imaging. J Bone Miner Res 2012;4:876–90.
[45] Quan BD, Sone ED. Structural changes in collagen fibrils across a mineralized interface revealed by cryo-TEM. Bone 2015;8:42–9.
[46] Joseph PO, Tim JW, Andrew M. The *in situ* conformation and axial location of the intermolecular cross-linked non-helical telopeptides of type I collagen. Structure 2000;8:137–42.
[47] Meier R, Tomizaki T, Schulze-Briese C, Baumann U, Stocker A. The molecular basis of vitamin E retention: structure of human alpha-tocopherol transfer protein. J Mol Biol 2003;3:725–34.
[48] Cole DJ, Paynea MC, Ciacchibc LC. Water structuring and collagen adsorption at hydrophilic and hydrophobic silicon surfaces. Phys Chem Phys 2009;11:11395–9.
[49] Fariss M, Pascoe G, Reed N, Vitamin E. Reversal of the effect of extracellular calcium on chemically induced toxicity in hepatocytes. Science 1985;227:751–3.
[50] Titley KC, Torneck CD, Ruse ND, Kmec D. Adhesion of a resin composite to bleached and unbleached human enamel. J Endodont 1993;3:112–5.
[51] Raut S, Karzuon B, Atef E. Using in situ Raman spectroscopy to study the drug precipitation inhibition and super saturation mechanism of Vitamin E TPGS from self-emulsifying drug delivery systems (SEDDS). J Pharm Biomed Anal 2015;10:121–7.
[52] Seseogullari-Dirihan R, Tjäderhane L, Pashley DH, Tezvergil-Mutluay A. Effect of ultraviolet A-induced crosslinking on dentin collagen matrix. Dent Mater 2015;10:1225–31.
[53] Nascimento FD, Minciotti CL, Geraldeli S, Carrilho MR, Pashley DH, Tay FR. Cysteine cathepsins in human carious dentin. J Dent Res 2011;90:506–11.
[54] Wu JH, Croft KD. Vitamin E metabolism. Mol Aspects Med 2007;5–6:437–52.
[55] Silver FH, Horvath I, Foran DJ. Mechanical implications of the domain structure of fibril forming collagens: comparison of the molecular and fibrillar flexibilities of the a-chains found in types I, II, and III collagen. J Theor Biol 2002;2:243–54.
[56] Morris M. Raman spectroscopy of bone and cartilage emerging raman applications and techniques in biomedical and pharmaceutical fields. In: Matousek P, Morris M, editors. Biological and Medical Physics, Biomedical Engineering. Berlin, Heidelberg: Springer; 2010.

[57] Gullekson C, Lucas L, Hewitt K, Kreplak L. Surface-sensitive Raman spectroscopy of collagen I fibrils. Biophys J 2011;7:1837–45.
[58] Shoulders MD, Raines RT. Collagen structure and stability. Annu Rev Biochem 2009;2:929–58.
[59] Toworfe GK, Composto RJ, Shapiro IM, Ducheyne P. Nucleation and growth of calcium phosphate on amine-, carboxyl- and hydroxyl-silane self-assembled monolayers. Biomater 2006;4:631–42.
[60] Ziskind D, Hasday M, Cohen SR, Wagner HD. Young's modulus of peritubular and intertubular human dentin by nano-indentation tests. J Struct Biol 2011;1:23–30.
[61] Nair AK, Gautieri A, Chang SW, Buehler MJ. Molecular mechanics of mineralized collagen fibrils in bone. Nat Commun 2013;7:1724.
[62] Stephanie VC, Helene F, Evelyne G, Jean-Paul R, Francoise M. Association between collagen cross-links and trabecular microarchitecture properties of human vertebral bone. BONE 2010;2:342–7.
[63] Traub W, Arad T, Weiner S. Three-dimensional ordered distribution of crystals in turkey tendon collagen fibers. Proc Natl Acad Sci U S A 1989;86:9822–6.
[64] Glimcher MJ. Mechanism of calcification: role of collagen fibrils and collagen phosphoprotein complexes in vitro and in vivo. Anat Rec 1989;224:139–53.
[65] Huesa C, Yadav MC, Finnil ä MA, Goodyear SR, Robins SP, Tanner KE. PHOSPHO1 is essential for mechanically competent mineralization and the avoidance of spontaneous fractures. Bone 2011;48:1066–74.
[66] Zhang Y, Sukthankar P, Tomich JM, Conrad GW. Effect of the synthetic NC-1059 peptide on diffusion of riboflavin across an intact corneal epithelium. Invest Ophthalmol Vis Sci 2012;53:2620–9.
[67] Shah AR, Banerjee R. Effect of D-alpha-tocopheryl polyethylene glycol 1000 succinate 781 (TPGS) on surfactant monolayers. Colloids Surf B Biointerfaces 2011;85:116–24.